Quantum Interference of Tunably Indistinguishable Photons from Remote Organic Molecules

R. Lettow,[1] Y. L. A. Rezus,[1] A. Renn,[1] G. Zumofen,[1] E. Ikonen,[2] S. Götzinger,[1] and V. Sandoghdar[1]

[1]*Laboratory of Physical Chemistry and optETH, ETH Zurich, CH-8093 Zurich, Switzerland*

[2]*Metrology Research Institute, Aalto University and Centre for Metrology and Accreditation (MIKES), P.O. Box 13000, FI-00076 Aalto, Finland*

(Received 11 November 2009; published 26 March 2010)

We demonstrate two-photon interference using two remote single molecules as bright solid-state sources of indistinguishable photons. By varying the transition frequency and spectral width of one molecule, we tune and explore the effect of photon distinguishability. We discuss future improvements on the brightness of single-photon beams, their integration by large numbers on chips, and the extension of our experimental scheme to coupling and entanglement of distant molecules.

DOI: 10.1103/PhysRevLett.104.123605 PACS numbers: 42.50.Dv, 03.67.Bg, 42.50.Ar, 42.50.Lc

Recent developments in quantum engineering have redrawn the attention of scientists to the phenomenon of interference between single photons [1–7] for its potential in applications such as entanglement generation [8] and optical quantum computing [9,10]. In a two-photon quantum interference (TPQI) experiment indistinguishable single photons from two beams enter the input ports of a 50:50 beam splitter and leave together in one of the output ports [11,12]. Ideally, it is desirable to use bright independent sources of Fourier-limited photons, and it turns out that single quantum emitters are predestined for this task because they are intrinsically small and can emit lifetime-limited photons one at a time [13]. Indeed, TPQI measurements have been successfully demonstrated using single atoms and ions in vacuum chambers [2,4,5]. However, atom reloading time, difficulties in efficient light collection, and scaling to large numbers of emitters pose major challenges to various realizations. Solid-state emitters such as semiconductor quantum dots and color centers are scalable on chips, can have large emission rates, and lend themselves to highly efficient collection schemes [14], but they usually face the hurdles of spectral dephasing and inhomogeneity. In this work, we show that organic molecules embedded in organic matrices master all these challenges and discuss the conditions for tolerating deviations from the ideal case.

The organic dye molecules in this study were dibenzanthanthrene (DBATT) embedded in *n*-tetradecane at a concentration of about 10^{-6} M. As illustrated in Fig. 1(a) and described in detail in Ref. [15], we used separate microscopes and samples to extract indistinguishable photons on the zero-phonon lines (ZPLs) of two remote molecules. At temperatures $T < 2$ K, DBATT displays a sharp lifetime-limited ZPL ($\gamma_0 \sim 17$ MHz) between the ground vibrational level of the electronic ground state $S_{0,v=0}$ and the ground vibrational level of the electronic excited state $S_{1,v=0}$ at 589 nm [see Fig. 1(b)] [16]. We used a narrowband (<1 MHz) dye laser to address molecules across the inhomogeneous spectral distribution of the sample (~2 THz) [17]. As the frequency of the laser was scanned, ZPLs of individual molecules were excited selectively, and we recorded the Stokes-shifted fluorescence on the $S_{1,v=0} \rightarrow S_{0,v\neq 0}$ transitions [see Fig. 1(b)] to detect each molecule [18]. To obtain the same ZPL frequency for two molecules in the two samples, we selected two molecules with resonances such that they could be tuned to each other by applying a voltage to the gold microelectrodes fabricated on the substrates [see Fig. 1(c)].

Once we had prepared two molecules with identical ZPLs, we generated Fourier-limited single photons from them by tuning the dye laser frequency to the transition between the ground state and the first vibrational level of the electronic excited state ($S_{1,v=1}$). We found that despite having the same ZPL, the $S_{0,v=0} \rightarrow S_{1,v=1}$ transition frequencies were typically not the same for the two selected molecules. Nevertheless, these transitions overlapped within their linewidths of about 30 GHz [15], allowing us to excite the two molecules equally strongly by a suitable adjustment of the laser frequency. The $S_{1,v=1}$ state rapidly relaxes to $S_{1,v=0}$. The latter has a lifetime of 9.5 ns due to a radiative decay to $S_{0,v=0}$ (ZPL) and $S_{0,v\neq 0}$ with a branching ratio of about 0.5 [see Fig. 1(b)]. The emission on the ZPL with a coherence length of about 3 m could yield up to about 1×10^6 counts per second on the detector after passing a bandpass filter to reject the excitation light and the Stokes-shifted fluorescence [15]. It is worth emphasizing that the transition dipole of the ZPL has a well-defined orientation with respect to the backbone of the molecular structure, leading to a linearly polarized emission.

To realize an arrangement for a TPQI measurement, the ZPL emissions of the two molecules were focussed into the two arms of a single-mode polarization-maintaining fiber beam splitter, which conveniently ensured spatial mode matching of the two beams [see Fig. 1(a)]. Two half-wave plates were used to align the input polarizations. The outputs of this device were directed to two avalanche photodiodes (APDs) connected to a time-to-amplitude converter. By performing start-stop measurements, we re-

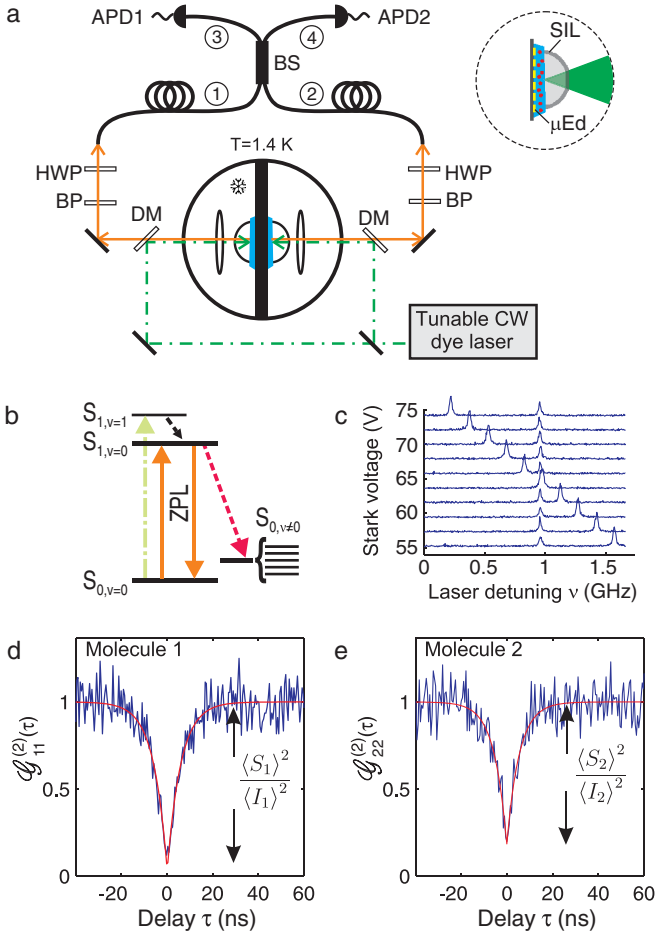

FIG. 1 (color online). (a) Schematics of the setup. DM, dichroic mirror; BS, beam splitter; BP, bandpass filter; HWP, half-wave plate; APD, avalanche photodiode; SIL, solid-immersion lens; μEd, gold microelectrodes. (b) Energy level diagram of a DBATT molecule. (c) Fluorescence excitation spectra of two selected molecules as a function of the voltage on the microelectrodes of one sample. This Stark effect was well described by the relation $\Delta\nu = 50 \times (V - 63)$ (with $\Delta\nu$ in MHz and V in Volts). (d, e) Intensity autocorrelation functions of the two molecules. The integration times corresponded to 3 min and 14 min at count rates of 34 and 16 kHz per APD, respectively. See text for the details of the theoretical fit.

corded intensity correlations with a time resolution of ~800 ps. In a first step, we always verified that each beam consisted of single photons by recording its intensity autocorrelation function $g^{(2)}(\tau) = \frac{\langle \hat{E}^-(t)\hat{E}^-(t+\tau)\hat{E}^+(t+\tau)\hat{E}^+(t)\rangle}{\langle \hat{E}^-(t)\hat{E}^+(t)\rangle^2}$ separately when the other fiber input was blocked. Here, τ denotes the time delay between the clicks on the two APDs. Figures 1(d) and 1(e) display strong photon antibunching at $\tau = 0$ for two molecules ($i = 1, 2$) from the two samples. In the ideal case, one expects $g_{ii}^{(2)}(0) = 0$ [19]. If the single-photon intensity (S_i) of each molecule is accompanied by an uncorrelated background (B_i), the overall detected intensity $I_i = S_i + B_i$ satisfies $\mathcal{G}_{ii}^{(2)}(\tau) = 1 + \frac{\langle S_i\rangle^2}{\langle I_i\rangle^2}[g_{ii}^{(2)}(\tau) - 1]$. In what follows, we use the calligraphic notation $\mathcal{G}(\tau)$ for a measurement in the presence of background and reserve $g(\tau)$ for the ideal correlation functions. The measured $\mathcal{G}_{ii}^{(2)}(0) = 1 - \frac{\langle S_i\rangle^2}{\langle I_i\rangle^2}$ values shown in Figs. 1(d) and 1(e) reveal that $\frac{\langle S\rangle}{\langle I\rangle} \geq 90\%$. In our experiment, the residual background stemmed from neighboring nonresonant molecules in the excitation spot, which can be eliminated by reducing the DBATT concentration during sample preparation.

For a beam consisting of single photons from two different molecules, $g^{(2)}(0)$ is reduced to 0.5 because the detection of a photon from one molecule does not impede detecting a second one from the other molecule [19]. The fascinating feature of TPQI is that even photons from two independent emitters can yield a perfect anticorrelation. Here, two photons that are indistinguishable in frequency, linewidth, spatial mode, and polarization enter the input arms of a beam splitter (labeled 1 and 2) and coalesce in one of the output ports (labeled 3 and 4), yielding a vanishing probability for the simultaneous detection of one photon in each arm [20]. The electric field operators in ports 3 and 4 are related to those in ports 1 and 2 according to [19]

$$\hat{E}_3^+(t) = \frac{1}{\sqrt{2}}(\hat{E}_2^+(t) + \hat{E}_1^+(t))$$
$$\hat{E}_4^+(t) = \frac{1}{\sqrt{2}}(\hat{E}_2^+(t) - \hat{E}_1^+(t)). \quad (1)$$

It is then straightforward to show that the theoretical expression for the intensity cross correlation function of the two outgoing modes becomes

$$\mathcal{G}_{34}^{(2)}(\tau) = c_1^2\mathcal{G}_{11}^{(2)}(\tau) + c_2^2\mathcal{G}_{22}^{(2)}(\tau) + 2c_1c_2 \times \left\{1 - \eta\frac{\langle S_1\rangle\langle S_2\rangle}{\langle I_1\rangle\langle I_2\rangle}|g_{11}^{(1)}(\tau)||g_{22}^{(1)}(\tau)|\cos(\Delta\omega\tau)\right\}, \quad (2)$$

where $c_i = I_i/(I_1 + I_2)$. The first and second terms represent the intensity autocorrelations of the individual sources as measured experimentally [see Figs. 1(d) and 1(e)], whereas the term in brackets originates from the mixed products of the two input intensities at frequency detuning $\Delta\omega$. For a quantum emitter i, the intensity (second order) and field (first order) autocorrelation functions are related according to $g_{ii}^{(2)}(\tau) = 1 - |g_{ii}^{(1)}(\tau)|^2$, where $g_{ii}^{(1)}(\tau) = e^{-i\omega_i\tau}e^{-\gamma|\tau|/2}$ and γ is the homogeneous linewidth of the emitter [19]. Thus, the measurements of $\mathcal{G}_{ii}^{(2)}$ determine both the ratios $\frac{\langle S_i\rangle}{\langle I_i\rangle}$ and $g_{ii}^{(1)}$, therefore fully characterizing $\mathcal{G}_{34}^{(2)}(\tau)$. In practice, the visibility of the two-photon interference could be reduced by factors other than the background light. We have accounted for this by including the phenomenological parameter $0 \leq \eta \leq 1$ in Eq. (2).

The blue trace in Fig. 2(a) displays $\mathcal{G}_{34}^{(2)}(\tau)$ when the inputs were photons emitted by the same two molecules

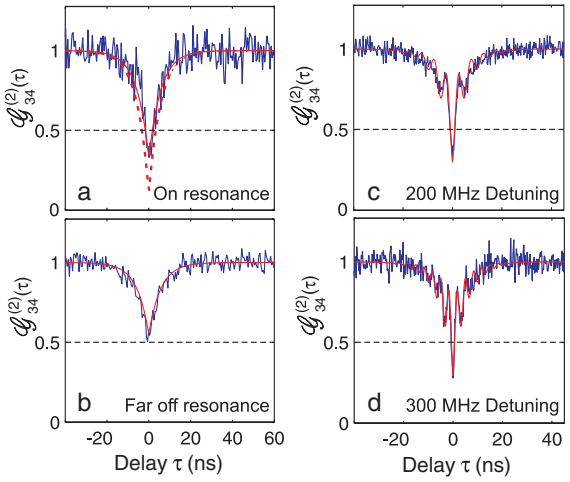

FIG. 2 (color online). (a) Intensity cross correlation function of photons with the same ZPL frequency exiting the output ports of the beam splitter. Integration time 9 min; count rate 27 kHz per APD. (b) Same as (a) if the ZPL of one molecule is frequency detuned by about 5 GHz (far-off resonant). Integration time 20 min; count rate 33 kHz per APD. (c),(d) Same as (a) if the two emitters are frequency detuned by 200 MHz and 300 MHz, respectively. The red curves are calculations based on Eqn. (2) with $\eta = 0.5$ (solid) and $\eta = 1$ (dashed), respectively. Integration times were 52 and 16 min, corresponding to count rate of 31 and 42 kHz per APD, respectively.

presented in Figs. 1(d) and 1(e). The fact that $\mathcal{G}^{(2)}_{34}(0) < 0.5$ well beyond the shot noise level at $\tau = 0$ is a clear proof of a quantum interference and has its origin in the corpuscular nature of single-emitter radiation [11,20]. The red curve shows a very good agreement with the predictions of Eq. (2) based on the measurements of $\mathcal{G}^{(2)}_{ii}(\tau)$ and with the assumption that $\eta = 0.5$. The origin of the contrast reduction was due to polarization ellipticities caused by a number of elements such as dielectric mirrors and cryostat windows. For comparison, the dashed red curve displays the prediction of calculations for $\eta = 1$. It is worth emphasizing that the data in Fig. 2(a) were recorded in only 9 min, more than 10 times faster than many of the previous efforts using single emitters [2,4,5].

To examine the impact of photon distinguishability on the cross correlation function, we exploited the frequency tunability of our emitters and changed the frequency of one molecule. First, we explored the case of far-off detuning by setting $\Delta\omega/2\pi \sim 5$ GHz. Figure 2(b) confirms that in this case we obtained $\mathcal{G}^{(2)}_{34}(0) \simeq 0.5$. The red curve shows a very good agreement with the outcome of calculation with no free parameters and assuming $\eta = 0$. The latter condition is justified by the fact that for photons with a large frequency difference, the term proportional to the cosine in Eq. (2) is washed out due to the limited time resolution of our detectors. At the same time, this term suggests that a frequency mismatch between the two emitters should introduce a time-dependent beat signal in the coincidence counts [2]. Figures 2(c) and 2(d) display the measured two-photon interference signal when the ZPL of one molecule was detuned by $\Delta\omega/2\pi = 200$ and 300 MHz, respectively. The solid red curves show that calculations based on $\eta = 0.5$ provide excellent agreement with the experimental findings. It is noteworthy that although the two photons are clearly distinguishable in frequency, we still find $\mathcal{G}^{(2)}_{34}(0) < 0.5$. This is because the measurement time resolution is better than $2\pi/\Delta\omega$, such that the information of the frequency difference is erased and the photons are rendered indistinguishable. Quantum beat signals shown in Figs. 2(c) and 2(d) were observed for the interference of delayed photons from a single atom [2], but to our knowledge, this is the first demonstration for photons from independent sources.

A key asset of organic molecules is that they routinely exhibit resonances with natural linewidth [13]. Although other solid-state systems such as quantum dots and color centers can, in principle, also reach this level of coherence, their performance has been critically dependent on the sample quality, and reports of Fourier-limited emission from these systems are still missing. Dephasing and spectral diffusion processes in solid-state emitters result in fast variations of the emitter resonance frequency and therefore fluctuations of $\Delta\omega$ in Eq. (2). As an example, Fig. 3(a) shows the theoretical predictions if the ZPL of one molecule were broadened to a full width at half-maximum (FWHM) of 2 GHz. Although we still find $g^{(2)}_{34}(0) = 0$, a finite detector time resolution of the order of 1 ns would

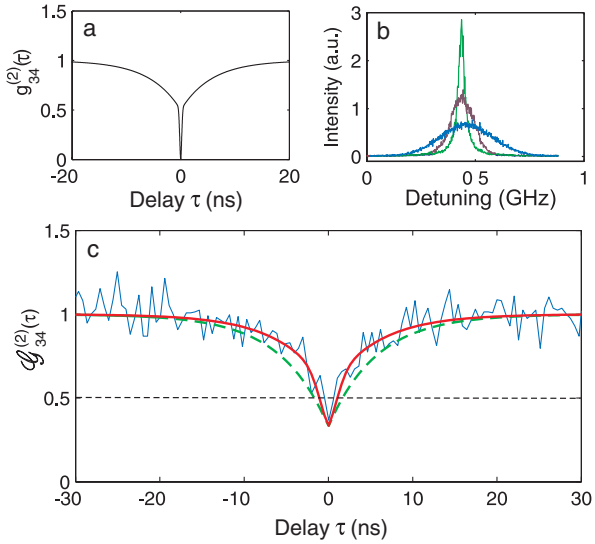

FIG. 3 (color online). (a) Theoretical prediction of the $g^{(2)}_{34}$ function when one molecule is broadened by about 120 times the natural linewidth γ_0. (b) Fluorescence excitation spectra of the ZPL for different noise amplitudes applied to the electrode. FWHM = 30 MHz (green), 120 (red), and 300 (blue). (c) Experimental measurement of the two-photon interference where the ZPL of one molecule was artificially broadened. The red solid curve is the prediction of Eq. (2) for $\eta = 0.5$ and the green dashed curve displays the data from Fig. 2(a). Integration time 7 min; count rate 28 kHz per APD.

wash out the contrast. In order to explore this experimentally, we artificially broadened the ZPL of one molecule by applying quasi-white noise to its sample electrodes. Figure 3(b) illustrates the resulting ZPL with FWHM = 300 MHz ($\sim 18\gamma_0$) at the maximum amplitude of the applied noise. We note in passing that the line profiles are no longer Lorentzian because of the limited modulation bandwidth of 1 MHz that was used in the Stark broadening process. The blue trace in Fig. 3(c) displays the resulting $\mathcal{G}^{(2)}_{34}(\tau)$ measurement, and the red solid curve shows the prediction of Eq. (2) with $\eta = 0.5$. As compared to the green curve which recasts the data of Fig. 2(a), the TPQI dip narrows but the contrast reduction is not substantial because the response of our detectors has been sufficiently fast. In summary, current photodetectors allow a considerable deviation of the spectral coherence from the ideal Fourier-limited condition without compromising the signature of the two-photon interference. Nevertheless, it has to be born in mind that any dephasing or spectral diffusion process reduces the probability of two-photon coalescence after the beam splitter because it lowers the coherence time of the photons ($1/\gamma$) with respect to the radiative lifetime ($1/\gamma_0$).

Other important and desirable features of single-photon sources for exploiting TPQI are high emission rates, large collection efficiency, and packaging of a large number of sources. Solid-state systems and, in particular organic molecules, promise to address all of these criteria at the same time. By excitation to the $S_{1,v=1}$ state via short pulses, DBATT can emit one photon per excited-state lifetime of 9.5 ns, thus reaching a rate of few tens of MHz at the ZPL frequency [21]. For an emitter at the interface of a medium with a high refractive index [see Fig. 1(a)], collection efficiencies beyond 90% can be achieved by optimizing the choices of the solid-immersion lens and the numerical aperture of the collecting lens [22]. Assuming a moderate collection efficiency of 50%, an overall detection efficiency (filters, detector quantum efficiency, etc.) of 10%, and a time bin of 10 ns, one arrives at a coincidence rate of $(10^7 \times 0.5 \times 0.1)^2 \times 10^{-8} > 10^3/\,\mathrm{sec}$ under pulsed excitation. Such a signal would provide a robust evidence of TPQI beyond the shot noise limit within a fraction of a second. Furthermore, one can integrate a large number of small solid-immersion lenses and independently addressable electrodes on the sample to extract many single-photon beams simultaneously [21].

Manipulation of Fourier-limited photons emitted by organic molecules paves the way towards a number of interesting experiments. First, our experimental setup can be readily used to perform coherent spectroscopy on one molecule with tunable single photons emitted by the second molecule [23]. Furthermore, the two-photon interference arrangement gives access to a conditional entanglement [24] of distant molecules. Although this entanglement only lasts during the lifetime of the electronic state, application of ultrafast pulses can allow a large number of coherent qubit rotations [25]. Moreover, one can envision replacing free-space photon channels used in our current experiment with on-chip dielectric waveguides [26] to realize ''hard-wired'' compact photonic circuits with many individually addressable single-photon sources.

We thank M. Pototschnig and J. Hwang for experimental help and R. Pfab and V. Ahtee for contribution to the initial phase of the experiment. This work was supported by the Swiss National Science Foundation (SNF) and ETH Zurich (Grant No. FEL-11-08-3 and the QSIT project Grant No. PP-01 07-02). E. I. acknowledges Grant No. 129971 from the Academy of Finland.

Note added.—We thank A. Bennett for informing us of their similar work with quantum dots [27] after our submission.

[1] C. Santori, D. Fattal, J. Vuckovic, G. S. Solomon, and Y. Yamamoto, Nature (London) **419**, 594 (2002).
[2] T. Legero, T. Wilk, M. Hennrich, G. Rempe, and A. Kuhn, Phys. Rev. Lett. **93**, 070503 (2004).
[3] A. Kiraz *et al.*, Phys. Rev. Lett. **94**, 223602 (2005).
[4] J. Beugnon *et al.*, Nature (London) **440**, 779 (2006).
[5] P. Maunz *et al.*, Nature Phys. **3**, 538 (2007).
[6] K. Sanaka, A. Pawlis, T. D. Ladd, K. Lischka, and Y. Yamamoto, Phys. Rev. Lett. **103**, 053601 (2009).
[7] A. J. Bennett, R. B. Patel, C. A. Nicoll, D. A. Ritchie, and A. J. Shields, Nature Phys. **5**, 715 (2009).
[8] Z. Y. Ou and L. Mandel, Phys. Rev. Lett. **61**, 50 (1988).
[9] E. Knill, R. Laflamme, and G. J. Milburn, Nature (London) **409**, 46 (2001).
[10] J. L. O'Brien, G. J. Pryde, A. G. White, T. C. Ralph, and D. Branning, Nature (London) **426**, 264 (2003).
[11] H. Paul, Rev. Mod. Phys. **58**, 209 (1986).
[12] C. K. Hong, Z. Y. Ou, and L. Mandel, Phys. Rev. Lett. **59**, 2044 (1987).
[13] B. Lounis and M. Orrit, Rep. Prog. Phys. **68**, 1129 (2005).
[14] W. Barnes *et al.*, Eur. Phys. J. D **18**, 197 (2002).
[15] R. Lettow *et al.*, Opt. Express **15**, 15842 (2007).
[16] C. Brunel, B. Lounis, P. Tamarat, and M. Orrit, Phys. Rev. Lett. **83**, 2722 (1999).
[17] W. E. Moerner and L. Kador, Phys. Rev. Lett. **62**, 2535 (1989).
[18] M. Orrit and J. Bernard, Phys. Rev. Lett. **65**, 2716 (1990).
[19] R. Loudon, *The Quantum Theory of Light* (Oxford University Press, Oxford, 2000).
[20] T. Legero, T. Wilk, A. Kuhn, and G. Rempe, Adv. At. Mol. Opt. Phys. **53**, 253 (2006).
[21] V. Ahtee *et al.*, J. Mod. Opt. **56**, 161 (2009).
[22] K. Koyama, M. Yoshita, M. Baba, T. Suemoto, and H. Akiyama, Appl. Phys. Lett. **75**, 1667 (1999).
[23] G. Wrigge, I. Gerhardt, J. Hwang, G. Zumofen, and V. Sandoghdar, Nature Phys. **4**, 60 (2008).
[24] D. L. Moehring *et al.*, Nature (London) **449**, 68 (2007).
[25] I. Gerhardt *et al.*, Phys. Rev. A **79**, 011402(R) (2009).
[26] Q. Quan, I. Bulu, and M. Loncar, Phys. Rev. A **80**, 011810 (R) (2009).
[27] R. B. Patel *et al.*, arXiv:0911.3997v1.